Subharmonics arising from the application of an electric field across a smectic-*C* liquid crystal

I. W. Stewart,[1] T. Carlsson,[2] and R. W. B. Ardill[3]
[1]*Department of Mathematics, University of Strathclyde, Livingstone Tower, 26 Richmond Street, Glasgow G1 1XH, Scotland*
[2]*Physics Department, Chalmers University of Technology, S-412 96 Göteborg, Sweden*
[3]*Department of Theoretical Mechanics, University of Nottingham, Nottingham NG7 2RD, England*

(Received 13 May 1996)

It was recently shown [I. W. Stewart, T. Carlsson, and F. M. Leslie, Phys. Rev. E **49**, 2130 (1994)] that chaotic instabilities can occur theoretically in planar samples of smectic-*C* liquid crystals. These instabilities were found by considering a special perturbation to the dynamic equation when a static electric field was augmented by a weak, slowly oscillating electric field across a sample of smectic-*C* liquid crystal. This analysis relied on a special traveling-wave solution of the dynamic equation. In this paper we show that there are also other solutions (subharmonics) with different boundary conditions that do not exhibit chaos and these solutions can be related to sample depth. An application of a Melnikov theory for subharmonics in the phase plane provides criteria for the existence of nonchaotic solutions to the specially perturbed dynamic equation. Such criteria involve the normalized frequency of the augmented field and its magnitude; the present analysis gives insight into the special previous results involving chaos and gives a general phase plane interpretation of solutions, confirming that both chaotic and nonchaotic behavior is possible, depending on the sample depth, boundary conditions, and properties of the augmented oscillating field. [S1063-651X(96)03812-3]

PACS number(s): 61.30 Cz

I. INTRODUCTION

Liquid crystals are generally composed of elongated molecules where the average long molecular axes locally align along one common direction in space described by a unit vector **n**, called the director. Smectic-*C* liquid crystals form layered structures in which the director **n** makes an angle θ with respect to the layer normal. We shall assume that θ is always some fixed constant. The unit layer normal is denoted by **a** and, as introduced by de Gennes [1], a unit vector **c** that is perpendicular to **a** describes the direction of the average molecular tilt of the sample with respect to the layer normal. The director **c** is the unit orthogonal projection of **n** onto the smectic planes. A complete description of the orientation of **n** in smectic liquid crystals can clearly be deduced from the knowledge of **a** and **c**. The orientation of **c** (and hence **n**) is known to be influenced by the application of electric fields [1–3], the result commonly being a Fréedericksz transition in the case of strong anchoring, which occurs when **c** begins to rotate around the layer normal while the layers remain intact. Static and moving domain walls that leave the layer structure undisturbed are also possible [4–6].

In [7] the existence of chaotic instabilities in the orientation of **c** (and hence the molecular axes) was theoretically demonstrated when a static electric field augmented by a weak, slowly oscillating field is applied across a sample of smectic liquid crystal arranged in parallel planar layers, this field making a small angle with the plane of the layers. Critical values for the onset of chaotic dynamics were found for the frequency and strength of the oscillating field and smectic tilt angle when reasonable approximations were made. The existence result presented in [7] made use of an explicit static field solution to the partial differential equation derived from the continuum theory of Leslie, Stewart, and Nakagawa [8]. Augmenting the static field with a weak, slowly oscillating field enabled a perturbation analysis to be carried out based on the known exact solution for the static field case. The resulting perturbed partial differential equation was transformed to a second-order nonlinear ordinary differential equation and the phase plane for this equation was shown to have separatrices (homoclinic orbits) that corresponded to the possible static field solutions. Melnikov's method (see [9]) was then employed to prove the existence of chaotic solutions whenever the initial data were chosen sufficiently close to the separatrices in the phase plane, that is, whenever the known exact solutions were perturbed by a suitable small oscillating field. It is the purpose of this article to complete a full analysis of the phase plane and examine the consequences for any initial data, not necessarily near the separatrices [7]. It will be shown that if the initial data are chosen far enough away from the separatrices, then perturbed periodic solutions do exist.

II. DESCRIPTION OF THE PROBLEM

In this section we summarize the equations derived in [7], where full details can be found. The essential governing equation is (2.19) below. A phase plane interpretation of special unperturbed solutions representing traveling domain walls is also introduced. Other unperturbed solutions that are periodic in the phase plane will be derived. These unperturbed orbits will form the basis for applying the subharmonic Melnikov method to Eq. (2.19) in order to determine the stability or persistence of perturbed periodic solutions to (2.19).

A. Basic equations

Consider a sample of nonchiral smectic-*C* liquid crystal in the bulk where the equidistant smectic layers lie parallel

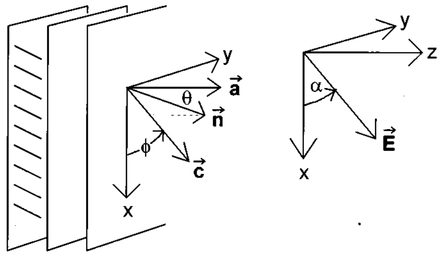

FIG. 1. Average molecular alignment described by the unit vector **n**, which makes an angle θ with the layer normal **a**. The director **c** is the unit vector parallel to the projection of the director **n** onto the smectic planes. The z axis coincides with the orientation of the layer normal **a** and the x and y axes lie within the smectic planes. The electric field **E** makes an angle α with the smectic planes as shown.

with the xy plane, the unit layer normal **a** being parallel to the z axis (see Fig. 1). The directors **a** and **c** are subject to the constraints

$$\mathbf{a}\cdot\mathbf{a}=\mathbf{c}\cdot\mathbf{c}=1, \quad \mathbf{a}\cdot\mathbf{c}=\mathbf{0} \tag{2.1}$$

and, since we assume there are no dislocations, **a** must further fulfill [10]

$$\nabla\times\mathbf{a}=\mathbf{0}. \tag{2.2}$$

An electric field **E** is applied across the sample at a small angle α to the plane of the layers

$$\mathbf{E}=E_0\left(1+\frac{\epsilon}{2}\cos(\omega\epsilon t)\right)(\cos\alpha,0,\sin\alpha). \tag{2.3}$$

Equation (2.3) corresponds to a static electric field (of magnitude E_0) that is gradually augmented by a small ac field having a slowly varying frequency $\omega\epsilon$ where ϵ is suitably small.

We make the following ansatz for **a**,**c**, and **n**:

$$\mathbf{a}=(0,0,1), \tag{2.4}$$

$$\mathbf{c}=(\cos\phi(z,t),\sin\phi(z,t),0), \tag{2.5}$$

$$\mathbf{n}=\mathbf{a}\cos\theta+\mathbf{c}\sin\theta, \tag{2.6}$$

where, as depicted in Fig. 1, the orientation of **c** within the layers is given by the phase angle $\phi(z,t)$. The resulting bulk energy density is given by [7]

$$w_{\mathrm{bulk}}=\frac{1}{2}B_3\left(\frac{\partial\phi}{\partial z}\right)^2. \tag{2.7}$$

Here B_3 is the positive elastic constant related to the rotation of the **c** director observed from layer to layer, **c** having the same uniform orientation within each individual layer (see [3] for more details). The electric free energy density is [1]

$$w_{\mathrm{elec}}=-\tfrac{1}{2}\epsilon_a\epsilon_0(\mathbf{n}\cdot\mathbf{E})^2, \tag{2.8}$$

where ϵ_0 is the permittivity of free space and ϵ_a is the dielectric anisotropy of the liquid crystal, assumed to be positive. We set

$$w=w_{\mathrm{bulk}}+w_{\mathrm{elec}}. \tag{2.9}$$

If it is assumed that $|\epsilon|\ll 1$, then we can use Eqs. (2.3)–(2.9) and the smectic continuum dynamic theory of Leslie, Stewart, and Nakagawa [8] to derive the dynamic equation

$$\begin{aligned}B_3\frac{\partial^2\phi}{\partial z^2}-2\lambda_5\frac{\partial\phi}{\partial t}-\epsilon_a\epsilon_0E_0^2[1+\epsilon\cos(\omega\epsilon t)]\\ \times(\sin\alpha\cos\theta+\cos\alpha\sin\theta\cos\phi)\cos\alpha\sin\theta\sin\phi=0.\end{aligned} \tag{2.10}$$

Here λ_5 is the viscosity coefficient related to the rotation of the director **n** around a ficticious cone whose semivertical angle equals the smectic tilt angle θ.

As shown in [7], to make Eq. (2.10) more tractable we assume that $0<\alpha\ll 1$ and

$$\epsilon=\xi\alpha \tag{2.11}$$

for some positive constant ξ, which is essentially related to the magnitude of the ac field. To simplify the equation further we introduce the typical length and time scales

$$\lambda=\frac{\sin\theta}{E_0}\left(\frac{\bar{B}_3}{\epsilon_a\epsilon_0}\right)^{1/2}, \tag{2.12}$$

$$t_0=2\lambda_5/\epsilon_a\epsilon_0E_0^2, \tag{2.13}$$

respectively, where we have used the fact that the elastic constant B_3 has a tilt angle dependence $B_3\sim\bar{B}_3\sin^2\theta$. The constant $\bar{B}_3$ is approximately the temperature-independent part of B_3 (see [3] for details). For mathematical convenience we introduce the rescaled frequency $\bar{\omega}$ as

$$\bar{\omega}=\frac{\omega\xi t_0}{\sin^2\theta}. \tag{2.14}$$

Motivated by the static field solutions discussed in [7,5], we investigate solutions of the form

$$\phi(z,t)=\phi(\tau), \tag{2.15}$$

$$\tau=\frac{z-z_0}{\lambda}-\frac{t}{t_0}\alpha\sin^2\theta, \tag{2.16}$$

where z_0 is an arbitrary point. Examining the behavior of solutions near z_0 means that we can further suppose

$$|z-z_0|<\frac{\alpha\lambda}{t_0\omega\xi}\sin^2\theta. \tag{2.17}$$

With the assumptions contained in Eqs. (2.11)–(2.17), Eq. (2.10) becomes

$$\frac{d^2\phi}{d\tau^2}+\alpha\frac{d\phi}{d\tau}=\alpha\cot\theta\sin\phi+\frac{1}{2}[1+\xi\alpha\cos(\bar{\omega}\tau)]\sin(2\phi), \tag{2.18}$$

which can be rewritten in the equivalent first-order system

$$\frac{d}{d\tau}\begin{pmatrix}\phi\\ v\end{pmatrix}=\begin{pmatrix}v\\ \frac{1}{2}\sin(2\phi)\end{pmatrix}+\alpha\begin{pmatrix}0\\ -v+\cot\theta\,\sin\phi+\frac{\xi}{2}\cos(\overline{\omega\tau})\sin(2\phi)\end{pmatrix}=\begin{pmatrix}f_1(\phi,v)\\ f_2(\phi,v)\end{pmatrix}+\alpha\begin{pmatrix}g_1(\phi,v,\tau)\\ g_2(\phi,v,\tau)\end{pmatrix}=\mathbf{f}(\phi,v)+\alpha\mathbf{g}(\phi,v,\tau), \tag{2.19}$$

where $v=d\phi/d\tau$ and, for ease of notation below, we have introduced the functions $\mathbf{f}(\phi,v)$ and $\mathbf{g}(\phi,v,\tau)$ as indicated.

In [7] it was demonstrated that Eq. (2.19) can exhibit chaotic dynamics whenever θ and $\overline{\omega}$ lie within certain ranges [dependent upon the fixed value of ξ in (2.12)]. Since the choice of z_0 is arbitrary it can be concluded that chaos may be present wherever the ac field is applied. Nevertheless, this result is based solely upon the fact that (2.19) can be considered as a special perturbation to the unperturbed $\alpha=0$ version of (2.19) for certain initial data lying on either of two separatrices in the phase plane representing traveling domain walls. A natural question to ask is whether or not it is possible to carry out a similar analysis for other orbits in the phase plane, corresponding to initial data that are not necessarily close to these separatrices. This requires the phase plane approach, which is discussed next.

B. The unperturbed phase plane

When $\alpha=0$ the solutions to (2.19) include the separatrices in the phase plane as shown in Fig. 2, which repeats itself every π. The arrow represents the direction of the solution in the phase plane as $\tau\to+\infty$ (this corresponds to $t\to-\infty$: reversing the arrows gives the $t\to+\infty$ behavior). Two such homoclinic orbits are possible, labeled $\mathbf{q}^1$ and $\mathbf{q}^{-1}$ as indicated in the figure. For $\alpha=0$ the exact expressions for these orbits are solutions to (2.19), namely,

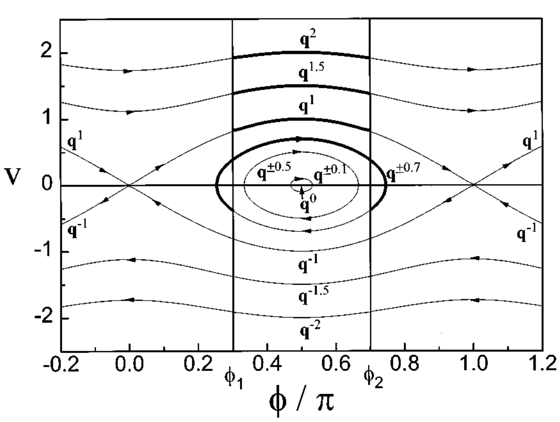

FIG. 2. Basic unperturbed phase plane (when $\alpha=0$) for Eq. (2.19). The orbits $\mathbf{q}^k(\phi,v)$ are shown for various values of the parameter k. For fixed boundary conditions $\phi=\phi_1,\phi_2$ the corresponding solutions are marked by the thick lines. The solutions matching these conditions are unique for $|k|>1$, but, as discussed in the text, there can be solutions corresponding to ''triple walls'' when $|k|<1$: here this is shown for $k=0.7$.

$$\mathbf{q}^1(\tau)=(\phi,v)=(2\,\tan^{-1}[\exp(\tau)],\,\text{sech}\,\tau)=(\cos^{-1}(-\tanh\tau),\,\text{sech}\,\tau), \tag{2.20}$$

$$\mathbf{q}^{-1}(\tau)=(\phi,v)=(\pi-2\,\tan^{-1}[\exp(\tau)],-\text{sech}\,\tau)=(\pi-\cos^{-1}(-\tanh\tau),-\text{sech}\,\tau). \tag{2.21}$$

$\mathbf{q}^{\pm1}$ represent walls that arise from the dielectric and elastic torques: these walls are known to be chaotically unstable for initial data chosen in the phase plane sufficiently close to either of the $\mathbf{q}^{\pm1}$ orbits [7].

At this point it is clear from Fig. 2 that other trajectories are available (labeled $\mathbf{q}^k$). These consist of two types of subharmonic periodic orbits, those between the separatrices and those outside the separatrices, as shown in the figure. Choosing initial data $(\phi(0),v(0))$ at any point then determines a solution to (2.19) when $\alpha=0$. Our analysis in the sections below depends on a perturbation to these known exact solutions.

At $\alpha=0$ the unperturbed system (2.19) has Hamiltonian H given by

$$H(\phi,v)=\tfrac{1}{2}v^2+\tfrac{1}{4}\cos(2\phi) \tag{2.22}$$

since

$$\frac{\partial H}{\partial v}=v,\quad -\frac{\partial H}{\partial\phi}=\frac{1}{2}\sin(2\phi). \tag{2.23}$$

To obtain the exact solutions for the subharmonics we consider the possibilities for H to be constant and set

$$H(\mathbf{q}^k(\tau))=\tfrac{1}{4}(2k^2-1)=h_k, \tag{2.24}$$

where k is a parameter, the form of h_k arising from the constant of integration and being chosen to simplify the notation used below. It turns out that k can be thought of as being related to the sample depth, as discussed in Sec. II C below. From (2.22) and (2.24)

$$\left(\frac{d\phi}{d\tau}\right)^2=k^2\left(1-\frac{1}{k^2}\cos^2\phi\right) \tag{2.25}$$

and therefore

$$\tau=\pm\frac{1}{k}\int_0^{\phi}\frac{d\eta}{\sqrt{1-\frac{1}{k^2}\cos^2\eta}}. \tag{2.26}$$

Some of the qualitative features of the phase plane represented in Fig. 2 will now be examined and related to the sample depth and existence of walls. We now examine the inner and outer subharmonics in the phase plane separately and adopt the notation of [11], p. 570 for the Jacobian elliptic functions.

C. Inner and outer subharmonics

1. Inner subharmonics: $0<|k|<1$, $\alpha=0$

For simplicity we only consider the plus sign in (2.26) since changing the sign of k gives the minus solution. In this case (2.26) becomes [12]

$$\tau=-F(\sin^{-1}[\cos(\phi)/k],k), \tag{2.27}$$

where F is the elliptic integral of the first kind. It follows that

$$\mathrm{sn}(-\tau,k)=\frac{\cos\phi}{k}, \tag{2.28}$$

where sn is the usual Jacobian elliptic function. Since sn is an odd function in τ, we finally have

$$\phi=\cos^{-1}[-k\ \mathrm{sn}(\tau,k)], \tag{2.29}$$

$$v=\frac{d\phi}{d\tau}=k\ \mathrm{cn}(\tau,k) \tag{2.30}$$

and note that (see [12], p. 48)

$$\sin\phi=\mathrm{dn}(\tau,k), \tag{2.31}$$

$$\cos\phi=-k\ \mathrm{sn}(\tau,k), \tag{2.32}$$

where cn and dn are Jacobian elliptic functions. Hence the inner subharmonic orbits are

$$\mathbf{q}^k=(\cos^{-1}[-k\ \mathrm{sn}(\tau,k)],\quad k\ \mathrm{cn}(\tau,k)), \tag{2.33}$$

with period [11]

$$T_k=4K(k), \tag{2.34}$$

where K is the complete elliptic integral of the first kind. From (2.33) we see that when $k=\pm 1$ we recover the separatrices (of infinite period) at (2.20) and (2.21) since [11]

$$\mathrm{sn}(\tau,\pm 1)=\tanh\tau, \tag{2.35}$$

$$\mathrm{cn}(\tau,\pm 1)=\mathrm{sech}\ \tau, \tag{2.36}$$

noting that π can be added to ϕ because the solutions repeat in the phase plane every π and $\cos^{-1}$ is an odd function. Since the $\mathbf{q}^k$ are periodic it is clear from (2.33) that we need to consider only $0<k<1$ in our analysis, the negative values of k generating the same orbits. Finally, $k=0$ in (2.33) gives the center point $(\pi/2,0)$.

2. Outer subharmonics: $|k|>1$, $\alpha=0$

As before, we choose the plus sign in (2.26): it will be shown that $k>1$ corresponds to the subharmonics above $\mathbf{q}^1$, while $k<-1$ corresponds to those below $\mathbf{q}^{-1}$. For $k>1$ we have from (2.26) (see [12], p. 176)

$$\tau=\frac{1}{k}F\left(\sin^{-1}\left[\frac{\sin\phi}{\sqrt{1-\frac{1}{k^2}\cos^2\phi}}\right],\frac{1}{k}\right) \tag{2.37}$$

and hence

$$\mathrm{sn}\left(k\tau,\frac{1}{k}\right)=\frac{\sin\phi}{\sqrt{1-\frac{1}{k^2}\cos^2\ \phi}}. \tag{2.38}$$

Noting that

$$\mathrm{dn}^2\left(\ ,\frac{1}{k}\right)+\left(\frac{1}{k^2}\right)\mathrm{sn}^2\left(\ ,\frac{1}{k}\right)=1\quad\text{for }|k|>1, \tag{2.39}$$

it then follows that for $k>1$ the subharmonics above $\mathbf{q}^1$ are

$$\begin{aligned}\mathbf{q}^k&=(\phi,v)\\&=\left(\sin^{-1}\left\{\sqrt{1-\frac{1}{k^2}}\ \mathrm{sd}\left[k\tau,\frac{1}{k}\right]\right\},\sqrt{k^2-1}\ \mathrm{nd}\left[k\tau,\frac{1}{k}\right]\right),\end{aligned} \tag{2.40}$$

with

$$\sin\phi=\sqrt{1-\frac{1}{k^2}}\ \mathrm{sd}\left(k\tau,\frac{1}{k}\right), \tag{2.41}$$

$$\cos\phi=\mathrm{cd}\left(k\tau,\frac{1}{k}\right). \tag{2.42}$$

Replacing k by $-k$ is equivalent to choosing the minus sign in (2.26). By repeating the above working, it is straightforward to show that for $k<-1$ the subharmonics below $\mathbf{q}^{-1}$ in Fig. 2 are

$$\begin{aligned}\mathbf{q}^k=(\phi,v)=&\left(\pi-\sin^{-1}\left\{\sqrt{1-\frac{1}{k^2}}\ \mathrm{sd}\left[k\tau,\frac{1}{k}\right]\right\},\right.\\&\left.-\sqrt{k^2-1}\ \mathrm{nd}\left[k\tau,\frac{1}{k}\right]\right),\end{aligned} \tag{2.43}$$

with

$$\sin\phi=\sqrt{1-\frac{1}{k^2}}\ \mathrm{sd}\left(k\tau,\frac{1}{k}\right), \tag{2.44}$$

$$\cos\phi=-\mathrm{cd}\left(k\tau,\frac{1}{k}\right). \tag{2.45}$$

The period of all the outer subharmonics with $|k|>1$ is [11]

$$T_k=\frac{4}{|k|}K\left(\frac{1}{k}\right). \tag{2.46}$$

Remark. It is clear from the above discussion and Fig. 2 that all the subharmonics $\mathbf{q}^k$ with periods T_k are continuous and fill the phase plane. Also, from (2.34) and (2.46), $T_k\to\infty$ monotonically as $k\to 1^-$ or 1^+. It is then straightforward to verify that all the necessary conditions are satisfied for an application of the Melnikov method outlined in [9], p. 185.

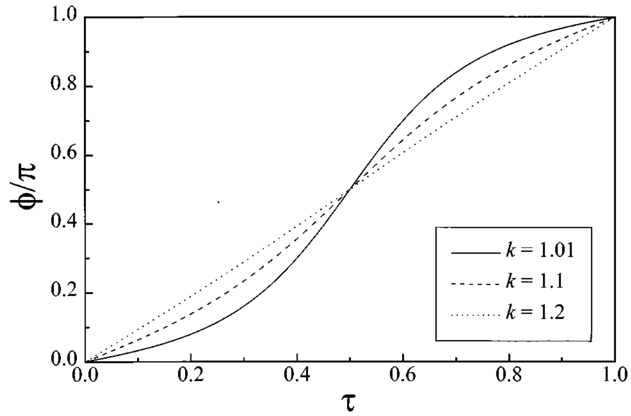

FIG. 3. For $k>1$ the sample depth d increases as k decreases to 1. If ϕ is to maintain its π wall as d increases then the wall width decreases and is centered around $\phi=\pi/2$. Here $\bar{\tau}$ is essentially the normalized rescaled variable that is related to the finite sample depth as discussed for Eq. (2.47) in the text.

D. Features of the phase plane related to sample thickness

In order to gain some insight into the role of the parameter k we can, for the moment, consider a sample of finite thickness and introduce the rescaled variable $\bar{\tau}$ defined by

$$\bar{\tau}=\frac{\tau}{\tau_{\max}}=\frac{1}{\tau_{\max}}\int_0^{\phi}\frac{d\eta}{\sqrt{k^2-\cos^2\eta}}, \tag{2.47}$$

$$\tau_{\max}=\int_0^{\pi}\frac{d\eta}{\sqrt{k^2-\cos^2\eta}}, \tag{2.48}$$

where for convenience the plus sign in (2.26) has been chosen and it is assumed that $k>1$. This corresponds to being in the upper half plane of periodic orbits in Fig. 2. It is then clear that v is never zero and hence there are no walls for $k>1$, there are only smeared out configurations. If the sample thickness is d and we suppose that the director is fixed at $\phi=0$ and π on the bounding surfaces then, from (2.12) and (2.16) (with $\alpha=0$ and $z_0=0$)

$$\tau_{\max}=\frac{d}{\lambda}=dE_0\left(\frac{\epsilon_a\epsilon_0}{\bar{B}_3}\right)^{1/2} \tag{2.49}$$

and therefore from (2.48) and (2.49) it is seen that k is related to the sample depth: as d increases, k decreases to 1. Figure 3 shows the effect of k upon the director phase angle ϕ for $k=1.2$, 1.1, and 1.01. As k decreases (i.e., as the sample depth d increases) the π walls are seen to develop a smaller wall width (the distance over $\bar{\tau}$ for which ϕ changes from $\pi/4$ to $3\pi/4$) centered around $\phi=\pi/2$. Also, as k increases the sample depth decreases. This is as expected since the thinner the sample is, the larger $d\phi/dz$ must be in order to facilitate a rotation of the c director through π across the sample. Physically, there is a competition between the elastic and electric torques. When $\lambda\ll d$, that is, the electric torque dominates over the elastic torque, then the c director will remain parallel to the field throughout most of the sample and one or more walls will appear depending on the boundary conditions imposed on the sample. For $\lambda\gg d$, for example, when the electric field is weak, that is, the elastic torque dominates over the electric torque, the c-director profile will be a slowly varying function. Equation (2.49) shows $\tau_{\max}$ to be a universal parameter linking d and λ for these solutions: for d/λ (or dE_0)=const, k can be calculated from (2.48) to give the relevant, unique trajectory in the phase plane in Fig. 2. When the boundary conditions are 0 and π then $\lambda\gg d$ corresponds to $k\to\infty$, while $\lambda\ll d$ corresponds to $k\to1^+$. All of this is expected from the physics of the problem and these results are evident from the mathematics in Eq. (2.48).

When $k=1$ we obtain the walls described and discussed in [7]. For $0<k<1$ there are solutions for ϕ that are of a similar nature to those discussed for $k>1$. In this case $\tau_{\max}$ needs to be suitably redefined (since the walls are no longer π reorientations of the c director). For symmetric boundary conditions, that is, $\phi_1=\pi/2-\delta$ and $\phi_2=\pi/2+\delta$ for $0<\delta<\pi/2$, the k value for the solutions will decrease with increasing value of the control parameter $\tau_{\max}=d/\lambda$ (increasing the sample thickness and /or the electric field). In the case of a very large electric field the trajectory may have to start and end in the lower half of the phase plane, ultimately corresponding, for example, to a ''triple wall'' when $k\sim1^-$ or $k\sim-1^+$, where $\tau_{\max}\sim\infty$. This information can be seen from Fig. 2: the thick lines on parts of the trajectory curves are such that the solutions match the boundary conditions marked at ϕ_1 and ϕ_2. For $k>1$ there is only one possible part of the trajectory that can be a solution. However, if $0<k<1$, then the solution ϕ can exhibit a triple wall by lying on a trajectory such as that shown in Fig. 2 when $k=0.7$. The phase angle ϕ will decrease from the boundary condition ϕ_1 to a minimum value and then increase to a maximum value (larger than ϕ_2) before decreasing to ϕ_2 as shown. Of course, as can be seen from Fig. 2, there is also a single wall solution with $\phi=\phi_1,\phi_2$ on the boundaries for $k=0.7$. The relevant solution depends on the derivatives of ϕ at the boundaries.

III. THE SUBHARMONIC MELNIKOV FUNCTION

Suppose the electric field is tilted to the layers (so that $\alpha\neq0$) and let $\mathbf{q}^k$ be a subharmonic orbit such that its period T_k satisfies the resonance condition

$$T_k=mT/n \tag{3.1}$$

for some relatively prime integers m and n (i.e., m and n have no common factor other than 1), where

$$T=\frac{2\pi}{\bar{\omega}}<\infty \tag{3.2}$$

denotes the period of the perturbation term in Eq. (2.19). We will see later that for the cases of interest we find that $n=1$ and m is an even integer. Define the wedge product of $\mathbf{f}$ and $\mathbf{g}$ by

$$\mathbf{f}\wedge\mathbf{g}=f_1g_2-f_2g_1. \tag{3.3}$$

The subharmonic Melnikov function for a $\mathbf{q}^k$ satisfying (3.1) is defined by

$$M_k^{m/n}(\tau_0)=\int_0^{mT}\mathbf{f}(\mathbf{q}^k(\tau))\wedge\mathbf{g}(\mathbf{q}^k(\tau),\tau+\tau_0)\,d\tau \quad (3.4)$$

and is said to have a simple zero at τ_1 if

$$M_k^{m/n}(\tau_1)=0,\quad \frac{d}{d\tau_0}M_k^{m/n}(\tau_1)\neq 0. \quad (3.5)$$

We now quote the following theorem from [9].

Theorem. Let h_k be as defined in Eq. (2.24). If (i) $M_k^{m/n}(\tau_0)$ has simple zeros and is independent of α and (ii) $dT_k/dh_k\neq 0$, then there is a constant $\alpha(n)$ depending only on n such that for $0<\alpha\leqslant\alpha(n)$ Eq. (2.19) has a perturbed subharmonic orbit of period mT.

This theorem will allow us to show that there exist perturbed periodic solutions for $\alpha\neq 0$ in (2.19) [and hence perturbed solutions to (2.10)] when the initial data lie off the separatrices (when $\alpha=0$). This is in contrast to the results of [7], where chaotic solutions are shown to occur if the initial data lie on $\mathbf{q}^{\pm 1}$ (at $\alpha=0$); other specific periodic solutions that satisfy the resonance condition (3.1) will persist (with perhaps different periods) after small perturbations. Periodic solutions in the variable τ represent time-dependent spatially periodic twisting of the c director throughout the sample in the z direction, the orientation of the director being uniform in each smectic layer. From (2.12), (2.16), (3.2), and the theorem, the perturbed period of such c-director orientations in the z direction will be

$$z_k=\lambda mT=\left(\frac{\overline{B_3}}{\epsilon_a\epsilon_0}\right)^{1/2}\frac{2m\pi}{\overline{\omega}E_0}. \quad (3.6)$$

Alternatively, if one observes the sample at a particular position z_1 say, then the time period for the twisted structure to be seen repeating itself at z_1 as time progresses, is from (2.13), (2.16), (3.2), and the theorem,

$$t_k=\frac{mTt_0}{\alpha\sin^2\theta}=\frac{4m\pi\lambda_5}{\alpha\epsilon_a\epsilon_0\overline{\omega}E_0^2\sin^2\theta}. \quad (3.7)$$

Here, of course, m is related to the initial data via the choice of subharmonic $\mathbf{q}^k$ satisfying (3.1). The range of α for which the results are valid depends on the constant $\alpha(n)$.

IV. EXISTENCE OF PERTURBED SUBHARMONICS

In this section we prove that there exist periodic solutions to Eq. (2.19) when $\alpha\neq 0$ is sufficiently small using the Melnikov theorem in Sec. III.

A. Perturbed inner subharmonics: $0<|k|<1$, $\alpha\neq 0$

As mentioned in Sec. II, it is sufficient to consider $0<k<1$. By (2.34), (3.1), and (3.2) the resonance condition forces

$$T_k=4K(k)=\frac{2m\pi}{n\overline{\omega}}. \quad (4.1)$$

From [12], $K(k)$ is a strictly monotonically increasing function with $\pi/2<K(k)<\infty$ and therefore Eq. (4.1) can be solved uniquely for each pair of relatively prime positive integers m and n to give $k=k(m,n)$, provided

$$\frac{m}{n}>\overline{\omega}. \quad (4.2)$$

This means that for any given $\overline{\omega}$, the numbers m and n can be chosen to satisfy Eq. (4.2), resulting in a unique $k(m,n)$ found from (4.1). This procedure leads to a unique unperturbed orbit $\mathbf{q}^{k(m,n)}(\tau)$ of period $T_{k(m,n)}$. The Melnikov method will show that such an orbit persists after small perturbations and the new orbit will have period $mT=2m\pi/\overline{\omega}$.

We now suppose that for a given $\overline{\omega}$ we have chosen m and n satisfying (4.2), leading to a unique $k(m,n)$ fulfilling (4.1). First, by (2.24) and (2.34)

$$\frac{dT_k}{dh_k}=\frac{dT_k}{dk}\left(\frac{dh_k}{dk}\right)^{-1}=\frac{4}{k}\frac{dK}{dk} \quad (4.3)$$

for any k and does not equal zero since K is strictly monotonically increasing. Therefore condition (ii) of the Melnikov theorem is satisfied. It only remains to calculate $M_{k(m,n)}^{m/m}(\tau_0)$.

For ease of notation write $k=k(m,n)$. From (3.1) and (4.1), $mT=nT_k=4nK(k)$, and hence from Eqs. (2.19) and (2.29)–(2.33),

$$\begin{aligned}M_{k(m,n)}^{m/n}(\tau_0)&=\int_0^{4nK}\mathbf{f}(\mathbf{q}^k(\tau))\wedge\mathbf{g}(\mathbf{q}^k(\tau),\tau+\tau_0)\,d\tau\\ &=\int_0^{4nK}v\bigg(-v+\cot\theta\sin\phi\\ &\qquad+\frac{\xi}{2}\cos[\overline{\omega}(\tau+\tau_0)]\sin(2\phi)\bigg)d\tau\\ &=I_1+\cot\theta I_2+\xi I_3,\end{aligned} \quad (4.4)$$

where

$$I_1=-\int_0^{4nK}v^2(\tau)\,d\tau, \quad (4.5)$$

$$I_2=\int_0^{4nK}v(\tau)\sin\phi\,d\tau, \quad (4.6)$$

$$I_3=\int_0^{4nK}v(\tau)\cos[\overline{\omega}(\tau+\tau_0)]\cos\phi\sin\phi\,d\tau. \quad (4.7)$$

Let E and $\overline{E}$ denote the complete and incomplete elliptic integrals of the second kind, respectively, and denote the usual Jacobian amplitude function by am. Observing that [12]

$$\overline{E}(\mathrm{am}(4nK,k),k)=\overline{E}(2n\pi,k)=4nE(k), \quad (4.8)$$

it follows from (2.30) and [11], p. 630, that

$$I_1=-k^2\int_0^{4nK}\mathrm{cn}^2(\tau,k)\,d\tau$$

$$=4n(1-k^2)K(k)-\overline{E(}\mathrm{am}(4nK,k),k)$$
$$=4n[(1-k^2)K(k)-E(k)]. \tag{4.9}$$

From (2.30) and (2.31) and the periodic properties of sn [11]

$$I_2=k\int_0^{4nK}\mathrm{cn}(\tau,k)\ \mathrm{dn}(\tau,k)d\tau=k\int_0^{4nK}\frac{d}{d\tau}\ \mathrm{sn}(\tau,k)d\tau=0. \tag{4.10}$$

The integral I_3 requires more extensive computations. From (2.30)–(2.32)

$$I_3=-k^2\int_0^{4nK}\cos[\overline{\omega}(\tau+\tau_0)]\mathrm{cn}(\tau,k)\mathrm{dn}(\tau,k)\mathrm{sn}(\tau,k)d\tau$$
$$=\frac{1}{2}\int_0^{4nK}\cos[\overline{\omega}(\tau+\tau_0)]\frac{d}{d\tau}\ \mathrm{dn}^2(\tau,k)\ d\tau$$
$$=\frac{1}{2}\{\mathrm{dn}^2(\tau,k)\cos[\overline{\omega}(\tau+\tau_0)]\}_0^{4nK}$$
$$+\frac{\overline{\omega}}{2}\int_0^{4nK}\sin[\overline{\omega}(\tau+\tau_0)]\ \mathrm{dn}^2(\tau,k)\ d\tau. \tag{4.11}$$

Since $\mathrm{dn}(0,k)=\mathrm{dn}(4nK,k)=1$ and, from (4.1), $4nK=2m\pi/\overline{\omega}$, the first term on the right-hand side of (4.11) is zero and hence, by the series representation for dn^2 (see [13], p. 286),

$$I_3=\frac{\overline{\omega}}{2}\int_0^{4nK}\sin[\overline{\omega}(\tau+\tau_0)]\left[\frac{E(k)}{K(k)}+\frac{\pi^2}{K^2(k)}\right.$$
$$\left.\times\sum_{j=1}^{\infty} j\ \cos\left(\frac{j\pi}{K(k)}\tau\right)\mathrm{csch}\left(\frac{j\pi K(k')}{K(k)}\right)\right]d\tau, \tag{4.12}$$

where $k'=\sqrt{1-k^2}$. Again, from (4.1), it follows that the E/K term in (4.12) is zero and so (4.12) can be rewritten as

$$I_3=2\frac{\overline{\omega}^3n^2}{m^2}\sum_{j=1}^{\infty} j\ \mathrm{csch}\left(2\frac{j\overline{\omega}n}{m}K(k')\right)$$
$$\times\int_0^{4nK}\sin[\overline{\omega}(\tau+\tau_0)]\cos\left(2\frac{j\overline{\omega}n}{m}\tau\right)d\tau. \tag{4.13}$$

From [11], p. 140, and (4.1) it can be verified that

$$\int_0^{4nK}\sin[\overline{\omega}(\tau+\tau_0)]\cos\left(2\frac{j\overline{\omega}n}{m}\tau\right)d\tau$$
$$=\begin{cases}0 & \text{if } j\neq\dfrac{m}{2n}\\ \dfrac{m\pi}{\overline{\omega}}\sin(\overline{\omega}\tau_0) & \text{if } j=\dfrac{m}{2n}.\end{cases} \tag{4.14}$$

For integers, $2j$ can only equal m/n with m and n relatively prime when $n=1$ and m is even. Consequently, (4.13) is

$$I_3=\begin{cases}\pi\overline{\omega}^2\ \mathrm{csch}[\overline{\omega}K(k')]\sin(\overline{\omega}\tau_0) & \text{if } n=1,\quad m \text{ is even}\\ 0 & \text{otherwise.}\end{cases} \tag{4.15}$$

It now finally follows from (4.4), (4.9), (4.10), and (4.15) that

$$M_{k(m,n)}^{m/n}(\tau_0)=\begin{cases}4[(1-k^2)K(k)-E(k)]+\xi\pi\overline{\omega}^2\sin(\overline{\omega}\tau_0)\mathrm{csch}[\overline{\omega}K(k')] & \text{if } n=1,\quad m \text{ is even} \quad (4.16a)\\ 4n[(1-k^2)K(k)-E(k)] & \text{otherwise.} \quad (4.16b)\end{cases}$$

From (4.16) it is clear that in order to find a suitable $\mathbf{q}^k$ on which to apply the Melnikov theorem we must have $n=1$ and m even. For a fixed $\overline{\omega}$ we begin by choosing m even with $m>\overline{\omega}$ [from by (4.2)] and solve Eq. (4.1) for the unique value of k between 0 and 1. This value of k is then inserted into (4.16a) to enable $M_k^{m/1}(\tau_0)$ to be evaluated. This procedure can be carried out numerically. As an example to show that there exist m and k such that $M_k^{m/1}$ has simple zeros we try $\xi=5.2$, $\overline{\omega}=2.5$, and $m=4$ and find that $k=0.9408$ to four decimal places. The resulting $M_k^{m/1}$ is plotted in Fig. 4. This figure shows that the Melnikov function obviously has simple zeros in τ_0 and therefore there exists a perturbed periodic subharmonic orbit of period $mT=T_k$: both the perturbed and unperturbed subharmonics have the same period since, in this case, $n=1$.

Physically, since $mT=T_k$, the spatial periodicity at (3.6) is unaffected, but the introduction of a time period via (3.7) means that the periodic alignment of the director travels in time. From (3.7), $t_k\to\infty$ as $\alpha\to 0^+$, that is, we recover the static (infinite period) solution. Also, from (3.7), as E_0 increases the time period decreases.

If $n\neq 1$ or m is odd, then (4.16b) holds and $M_k^{m/n}$ cannot have simple zeros. This means that perturbed orbits have no fixed points and that they must move either inward or outward across the unperturbed orbit (see [9], p. 196).

B. Perturbed outer subharmonics: $|k|>1$, $\alpha\neq 0$

We shall only consider the case $k>1$: as mentioned below, the Melnikov function for $k<-1$ is identical. From (2.46), (3.1), and (3.2) the resonance condition in this case is

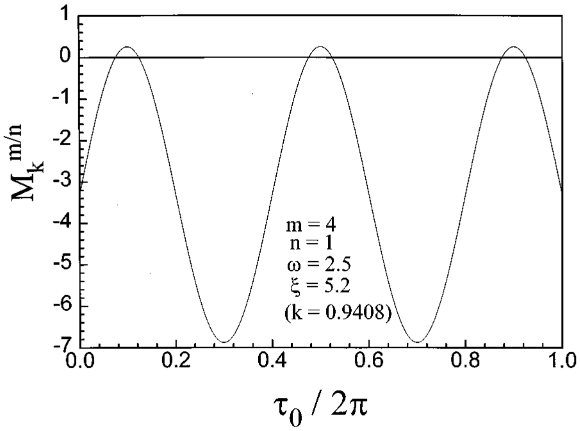

FIG. 4. Plot of the inner subharmonic Melnikov function $M_k^{m/n}(\tau_0)$ given by Eq. (4.16) for the particular values indicated in the figure. It is clear that it has simple zeros; this indicates the existence of perturbed periodic solutions when the angle α between the **E** field and the smectic planes is sufficiently small, as discussed in the text.

$$T_k = \frac{4}{k} K\left(\frac{1}{k}\right) = \frac{2m\pi}{n\overline{\omega}}. \tag{4.17}$$

From [12], T_k is a monotonically decreasing function in k and $0 < T_k < \infty$. Hence, for $\overline{\omega} > 0$ any relatively prime positive integers m and n can be inserted into (4.17) to solve for a unique $k = k(m,n)$ [this is in contrast to the restriction imposed at Eq. (4.2) for the inner subharmonics]. For any given $\overline{\omega}$ we can then always find a unique perturbed orbit $\mathbf{q}^{k(m,n)}(\tau)$ of period $T_{k(m,n)}$.

We now suppose that we have solved (4.17) for $k = k(m,n)$ for given $\overline{\omega}$ and relatively prime m and n. From (2.24) and (2.46)

$$\frac{dT_k}{dh_k} = \frac{dT_k}{dk}\left(\frac{dh_k}{dk}\right)^{-1} = -\frac{4}{k^3}\left[\frac{\dot{K}\left(\frac{1}{k}\right)}{k} + K\left(\frac{1}{k}\right)\right], \tag{4.18}$$

where the overdot denotes $d/d(1/k)$. Equation (4.18) is never zero since K and $\dot{K}$ are always positive for $k > 1$ (see [11], p. 905) and therefore condition (ii) of the Melnikov theorem is satisfied. As in Sec. IV A, it only remains to calculate $M_{k(m,n)}^{m/n}(\tau_0)$. From (3.1) and (4.17)

$$mT = nT_k = \frac{4n}{k} K\left(\frac{1}{k}\right), \tag{4.19}$$

and therefore from Eqs. (2.19) and (2.40)–(2.42) the Melnikov function is again provided by Eq. (4.4), except that in this case we replace I_1, I_2, and I_3, respectively, by

$$J_1 = -\int_0^{(4n/k)K(1/k)} (k^2 - 1)\ \mathrm{nd}^2\left(k\tau, \frac{1}{k}\right) d\tau, \tag{4.20}$$

$$J_2 = \int_0^{(4n/k)K(1/k)} \left(k - \frac{1}{k}\right) \mathrm{sn}\left(k\tau, \frac{1}{k}\right) \mathrm{nd}^2\left(k\tau, \frac{1}{k}\right) d\tau, \tag{4.21}$$

$$J_3 = \int_0^{(4n/k)K(1/k)} \left(k - \frac{1}{k}\right) \cos[\overline{\omega}(\tau + \tau_0)] \times \mathrm{sn}\left(k\tau, \frac{1}{k}\right) \mathrm{cn}\left(k\tau, \frac{1}{k}\right) \mathrm{nd}^3\left(k\tau, \frac{1}{k}\right) d\tau. \tag{4.22}$$

The first of these integral can be evaluated via [11], Eqs. 16.26.6 and 17.4.6, to give

$$J_1 = -4nkE\left(\frac{1}{k}\right), \tag{4.23}$$

while straightforward computations using [12], Eq. 5.137.2, show

$$J_2 = 0. \tag{4.24}$$

The integral J_3 is equivalent to

$$J_3 = \frac{1}{2}(k^2 - 1)\int_0^{4nK(1/k)} \cos[\overline{\omega}(u/k + \tau_0)]\ \frac{d}{du} \times \left(\frac{1}{\mathrm{dn}^2\left(u, \frac{1}{k}\right)}\right) du. \tag{4.25}$$

Since

$$\mathrm{dn}\left[u + K\left(\frac{1}{k}\right)\right] = \frac{\sqrt{k^2 - 1}}{k\ \mathrm{dn}\left(u, \frac{1}{k}\right)}, \tag{4.26}$$

we can use the series for dn^2 [13] with a further integration by parts, using (4.17) when necessary, to yield

$$J_3 = \frac{\overline{\omega}}{2}\int_0^{4nK(1/k)} \sin[\overline{\omega}(u/k + \tau_0)] \left[\frac{kE\left(\frac{1}{k}\right)}{K\left(\frac{1}{k}\right)} + \frac{k\pi^2}{K^2\left(\frac{1}{k}\right)} \sum_{j=1}^{\infty} (-1)^j \frac{j\cos\left[j\pi u / K\left(\frac{1}{k}\right)\right]}{\sinh\left[j\pi K\left(\sqrt{1 - \frac{1}{k^2}}\right) \Big/ K\left(\frac{1}{k}\right)\right]}\right] du. \tag{4.27}$$

The first term in (4.27) is zero and from [12], p. 140,

$$\int_0^{4nK} \sin[\overline{\omega}(u/k+\tau_0)]\cos(j\pi u/K)\ du = \begin{cases} 0 & \text{if } j \neq \dfrac{m}{2n} \\ 2nK\left(\dfrac{1}{k}\right)\sin(\overline{\omega}\tau_0) & \text{if } j = \dfrac{m}{2n}. \end{cases} \tag{4.28}$$

As in Sec. IV A, $2j$ can only equal m/n with m and n relatively prime when $n=1$ and m is even. Consequently, with the aid of (4.1),

$$J_3 = \begin{cases} (-1)^{m/2}\pi\overline{\omega}^2 \operatorname{csch}\left[\overline{\omega}K\left(\sqrt{1-\dfrac{1}{k^2}}\right) \Big/ k\right]\sin(\overline{\omega}\tau_0) & \text{if} \quad n=1, \quad m \text{ is even} \\ 0 \quad \text{otherwise.} \end{cases} \tag{4.29}$$

Hence from (4.1), (4.23), (4.24), and (4.29)

$$M^{m/n}_{k(m,n)}(\tau_0) = \begin{cases} -4nkE\left(\dfrac{1}{k}\right) + (-1)^{m/2}\xi\pi\overline{\omega}^2\sin(\overline{\omega}\tau_0)\operatorname{csch}\left[\overline{\omega}K\left(\sqrt{1-\dfrac{1}{k^2}}\right)\Big/ k\right] & \text{if } n=1, \quad m \text{ is even} \\ -4nkE\left(\dfrac{1}{k}\right) \quad \text{otherwise.} \end{cases} \tag{4.30}$$

In a similar way to the inner subharmonics, Eq. (4.30) shows that the Melnikov theorem can be applied when $n=1$ and m is even. As mentioned earlier, in this case there is no restriction such as that at (4.2) and therefore we can set $n=1$ and choose any even m. This will lead to a unique $k=k(m,1)>1$ for any given $\overline{\omega}>0$, via Eq. (4.17). Figure 5 shows $M_k^{m/1}$ when $\xi=10$, $\overline{\omega}=2.8$, and $m=6$, resulting in $k=1.0093$ to four decimal places. Clearly, in this particular example $M_k^{m/1}(\tau_0)$ has simple zeros in τ_0 and hence there exists a perturbed periodic subharmonic orbit of period $mT=T_k$. As before, both the perturbed and unperturbed subharmonics have the same period since $n=1$. The comments in the last two paragraphs of Sec. IV A equally apply to the outer subharmonics.

For $k=-1$ Eqs. (2.43)–(2.45) lead to analogous integrals in (4.20)–(4.22). It is easily verified that the period mT is the same and the Melnikov function is exactly that given by (4.30).

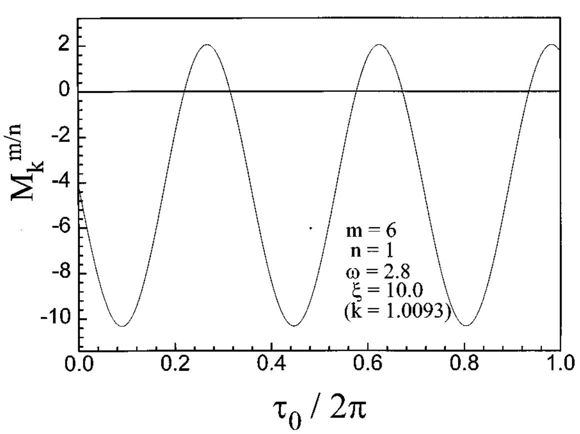

FIG. 5. Plot of the outer subharmonic Melnikov function $M_k^{m/n}(\tau_0)$ given in Eq. (4.30) for the values indicated in the figure. As in Fig. 4, the existence of perturbed periodic orbits is indicated by the presence of simple zeros, as mentioned in the text.

C. Remarks on the parameters ξ and $\overline{\omega}$

From Eqs. (4.16) and (4.30) it is possible to construct simultaneous values of ξ and $\overline{\omega}$ for which $M_k^{m/1}$ has simple zeros for either of the perturbed inner or outer subharmonics. For the inner subharmonics $(0<k<1)$ we note that $(1-k^2)K(k)-E(k)$ is an even function of k and is strictly monotonically increasing for $0\leqslant k\leqslant 1$, achieving its maximum value of 1; $\operatorname{csch}[\overline{\omega}K(k')]$, for fixed $\overline{\omega}$, is also strictly monotonically increasing on the same interval of k. For $M_k^{m/1}$ to have simple zeros we require that $\xi>\xi^{\text{in}}_{\text{min}}$, where

$$\xi^{\text{in}}_{\text{min}} = \frac{4}{\pi\overline{\omega}^2}[E(k)-(1-k^2)K(k)]\ \sinh(\overline{\omega}K(k')). \tag{4.31}$$

Further, from (4.1), we have, for $n=1$,

$$\overline{\omega} = \frac{m\pi}{2K(k)} \tag{4.32}$$

and therefore, provided $\xi>\xi^{\text{in}}_{\text{min}}$, we can find combinations of $\overline{\omega}$ and k such that (4.32) holds for a given value of m. Using expansions for $K(k)$ given in [12], we can show that for $n=1$

$$\overline{\omega}\to m \quad \text{as} \quad k\to 0^+, \tag{4.33}$$

$$\overline{\omega}\to 0 \quad \text{as} \quad k\to 1^-. \tag{4.34}$$

In a similar way, we can obtain results for the outer subharmonics $(1<k<\infty)$. From Eq. (4.30) it is seen that in this case the Melnikov function can only have simple zeros when $\xi>\xi^{\text{out}}_{\text{min}}$, where

$$\xi^{\text{out}}_{\text{min}} = \frac{4kE\left(\dfrac{1}{k}\right)}{\pi\overline{\omega}^2}\sinh\left\{\frac{\overline{\omega}}{k}K\left(\sqrt{1-\left[\frac{1}{k}\right]^2}\right)\right\}. \tag{4.35}$$

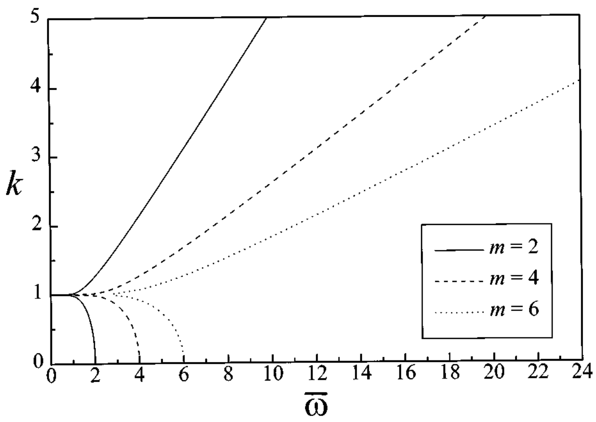

FIG. 6. Curves represent the combinations of $\overline{\omega}$ and k, which ensure simple zeros of the Melnikov function $M_k^{m/1}$, provided $\xi > \xi_{\min}$. Here $n=1$ and m takes the values indicated in the figure. For a given $\overline{\omega}$, the corresponding k and m provide the corresponding $\xi_{\min}$, which can be found from Eqs. (4.31) and (4.32) or Eqs. (4.35) and (4.36).

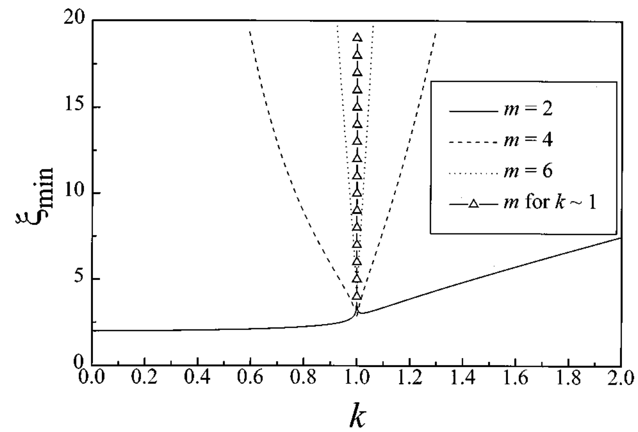

FIG. 7. Once k and m have been determined for a given $\overline{\omega}, \xi_{\min}$ can be calculated from Eqs. (4.31) or (4.35). $\xi_{\min}$ is shown for the values indicated. From Eqs. (4.39) and (4.40), $\xi_{\min} \to \infty$ as $k \to 1$ for all values of m; this is indicated by the triangle-dashed line.

Further, from (4.17) with $n=1$,

$$\overline{\omega} = \frac{\pi}{2} \frac{mk}{K\left(\frac{1}{k}\right)}. \tag{4.36}$$

As before, we can calculate combinations of $\overline{\omega}$ and k when $n=1$, which ensure that $M_k^{m/1}$ has simple zeros for various choices of suitable m, provided $\xi > \xi_{\min}^{\text{out}}$. Using expansions similar to those above, we find that

$$\overline{\omega} \to 0 \quad \text{as} \quad k \to 1^+, \tag{4.37}$$

$$\overline{\omega} \sim mk \quad \text{as} \quad k \to \infty. \tag{4.38}$$

The results of this section are summarized in Figs. 6 and 7. In Fig. 6 the combinations of $\overline{\omega}$ and k that ensure simple zeros of the Melnikov function are plotted for the special cases of $m=2$, 4, and 6, this figure being applicable for $0 \leqslant \overline{\omega}$, $k < \infty$. Figure 7 is a plot of $\xi_{\min}$ against k whenever (4.32) or (4.36) holds in the cases of $m=2$, 4, or 6; $\xi_{\min}$ actually tends to $+\infty$ for any m as $k \to 1$, as can be seen from the expansions [12] for $K(k)$ and $E(k)$:

$$\xi_{\min}^{\text{in}} \sim \frac{4}{m\pi} \ln\left(\frac{4}{\sqrt{1-k^2}}\right) \to \infty \quad \text{as} \quad k \to 1^-, \tag{4.39}$$

$$\xi_{\min}^{\text{out}} \sim \frac{4}{m\pi} \ln\left(\frac{4k}{\sqrt{k^2-1}}\right) \to \infty \quad \text{as} \quad k \to 1^+. \tag{4.40}$$

This divergence at $k=1$ is indicated by the triangle-dashed line in Fig. 7.

If we are given a frequency $\overline{\omega}$, then Fig. 6 will provide relevant values of m and k (related to the sample depth as discussed above) for the resonant subharmonics. These values of m and k can be inserted into Fig. 7 to find the value of $\xi_{\min}$. As examples, we can return to Figs. 4 and 5 and use Figs. 6 and 7 to see that the displayed values for m, k, $\overline{\omega}$, and ξ are all sufficient for the existence of subharmonics since $\xi > \xi_{\min}$ in each case.

V. DISCUSSION

We have shown that there are nonchaotic solutions for the problem outlined in Sec. II above when we consider a special perturbation to the dynamic equation (2.10), which leads to the governing equation (2.18). Unperturbed solutions (obtained when the angle α between the electric field and the smectic planes is zero) are parametrized in the phase plane (Fig. 2) by the variable k, which is related to the initial data, boundary conditions, and sample depth, as discussed is Sec. II D. These unperturbed (phase plane) solutions are employed via a Melnikov analysis to deduce whether or not there exists chaos in the possible solutions for small $\alpha \neq 0$. The case of $k=1$ was shown in a previous article [7] to result in chaotic solutions to the dynamic equation (2.18), which is in contrast to the results presented here where nonchaotic perturbed solutions are proved to exist when $k \neq 1$ and the frequency $\overline{\omega}$ and magnitude ξ of the augmented field satisfy the criteria displayed in Figs. 4–7. Depending on the boundary conditions, the conditions for such solutions to exist are essentially determined from Eqs. (4.16) and (4.30). Some special cases were displayed in Figs. 4 and 5, which show that the subharmonic Melnikov function can satisfy the requirements of the theorem stated in Sec. III above for the existence of perturbed solutions. The case where $k=1$ is shown to be special and relates to an infinite sample of smectic liquid crystal. That $k=1$ is unusual is again highlighted by the remarks in Sec. IV C, where $\xi_{\min}$ diverges for $k \to 1$; this warrants the separate treatment contained in [7]. The analysis here for $k \neq 1$ is shown to be qualitatively different from that in [7].

We hope that the results presented in this article will encourage more investigations of stability and instability in smectic-C liquid-crystal samples across which electric fields are applied.

[1] P.G. de Gennes, *The Physics of Liquid Crystals* (Clarendon, Oxford, 1974).
[2] A. Rapini, J. Phys. (Paris) **33**, 237 (1972).
[3] T. Carlsson, I.W. Stewart, and F.M. Leslie, Liq. Cryst. **9**, 661 (1991).
[4] I.W. Stewart and N. Raj, Mol. Cryst. Liq. Cryst. **185**, 47 (1990).
[5] P. Schiller, G. Pelzl, and D. Demus, Liq. Cryst. **2**, 21 (1987).
[6] Z. Zou, N.A. Clark, and T. Carlsson, Phys. Rev. E **49**, 3021 (1994).
[7] I.W. Stewart, T. Carlsson, and F.M. Leslie, Phys. Rev. E **49**, 2130 (1994).
[8] F.M. Leslie, I.W. Stewart, and M. Nakagawa, Mol. Cryst. Liq. Cryst. **198**, 443 (1991).
[9] J. Guckenheimer and P. Holmes, *Nonlinear Oscillations, Dynamical Systems, and Bifurcations of Vector Fields* (Springer-Verlag, New York, 1983).
[10] C.W. Oseen, Trans. Faraday Soc. **29**, 883 (1933).
[11] *Handbook of Mathematical Functions*, edited by M. Abramowitz and I.A. Stegun (Dover, New York, 1972).
[12] I.S. Gradshteyn and I.M. Ryzhik, in *Table of Integrals, Series and Products*, edited by A. Jeffrey (Academic, San Diego, 1980).
[13] A.G. Greenhill, *The Applications of Elliptic Functions* (MacMillan, London, 1892).